Research Paper

Excessive expression of miR-1a by statin causes skeletal injury through targeting mitogen-activated protein kinase kinase kinase 1

Chang-Ning Fu[1,2], Jia-Wen Song[1], Zhi-Peng Song[1], Qian-Wen Wang[1], Wen-Wu Bai[1], Tao Guo[1], Peng Li[3], Chao Liu[4], Shuang-Xi Wang[1,3,4], Bo Dong[2]

[1]The Key Laboratory of Cardiovascular Remodeling and Function Research, Chinese Ministry of Education, Chinese National Health Commission and Chinese Academy of Medical Sciences, The State and Shandong Province Joint Key Laboratory of Translational Cardiovascular Medicine, Department of Cardiology, Qilu Hospital, Cheeloo College of Medicine, Shandong University, Jinan, China
[2]Department of Cardiology, Shandong Provincial Hospital, Shandong University, Jinan, China
[3]Henan International Joint Laboratory of Cardiovascular Remodeling and Drug Intervention, School of Pharmacy, Xinxiang Medical University, Xinxiang, China
[4]Hubei Key Laboratory of Diabetes and Angiopathy, Hubei University of Science and Technology, Xianning, China

Correspondence to: Bo Dong, Shuang-Xi Wang, Chao Liu; **email:** bodong@sdu.edu.cn, shuangxiwang@sdu.edu.cn, liuchao@hbust.edu.cn
Keywords: statin, microRNA-1a, mitogen-activated protein kinase kinase kinase 1, apoptosis, myopathy
Received: November 5, 2020 **Accepted:** February 16, 2021 **Published:** April 16, 2021

ABSTRACT

Backgrounds: A major side effect of statin, a widely used drug to treat hyperlipidemia, is skeletal myopathy through cell apoptosis. The aim of this study is to investigate the roles of microRNA in statin-induced injury.
Methods: Apolipoprotein E knockout (ApoE-/-) mice were administered with simvastatin (20 mg/kg/day) for 8 weeks. Exercise capacity was evaluated by hanging grid test, forelimb grip strength, and running tolerance test.
Results: In cultured skeletal muscle cells, statin increased the levels of miR-1a but decreased the levels of mitogen-activated protein kinase kinase kinase 1 (MAP3K1) in a time or dose dependent manner. Both computational target-scan analysis and luciferase gene reporter assay indicated that MAP3K1 is the target gene of miR-1a. Statin induced cell apoptosis of skeletal muscle cells, but abolished by downregulating of miR-1a or upregulation of MAP3K1. Further, the effects of miR-1a inhibition on statin-induced cell apoptosis were ablated by MAP3K1 siRNA. In ApoE-/- mice, statin induced cell apoptosis of skeletal muscle cells and decreased exercise capacity in mice infected with vector, but not in mice with lentivirus-mediated miR-1a gene silence.
Conclusion: Statin causes skeletal injury through induction of miR-1a excessive expression to decrease MAP3K1 gene expression.

INTRODUCTION

Statins are widely used to treat hyperlipidemia and lower cardiovascular disease risks because they inhibit HMG-CoA reductase [1]. Statin also produces multiple side effects, such as muscle symptoms, diabetes mellitus, abdominal aortic aneurysm, and central nervous system complaints, limiting the applications in some patients [2, 3]. As for muscle symptoms, it includes statin-associated myalgia, rhabdomyolysis and necrotizing autoimmune myopathy, etc, in which the apoptosis of skeletal muscle cell plays critical roles [4, 5]. The molecular mechanism of skeletal muscle cell apoptosis needs further investigation.

MicroRNAs are approximately 20-nucleotide, single-stranded RNA molecules by targeting the 3′ untranslated regions (3′-UTR) of specific mRNAs

through partial complementarity [6]. In this way, miRNAs regulate gene expressions through inhibition of translation or transcript degradation. Interestingly, we have reported that statin inhibits miR-133a, specifically and highly expressed in skeletal and cardiac muscles, and ectopically expressed in endothelial cells under pathophysiological conditions [7, 8]. This demonstrates that statin is able to regulate myo-miRNA gene expressions.

As previously reported, miR-103/107, miR-208 and miR-21 are biomarkers of skeletal muscle toxicity [9], which are involved in myocyte apoptosis [10, 11], indicating several miRNAs are critical in the regulation of muscle cell function and fate determination. Some studies have demonstrated that overexpression of muscle-specific microRNAs, such as miR-1, leads to cell apoptosis and regulates skeletal muscle development [12–14]. Whether miR-1a is related to statin-induced skeletal injury remains unclear.

Based on aforementioned observations, we tested the hypothesis that statin causes skeletal injury through miR-1a-mediated of cell apoptosis. Here we reported that mitogen-activated protein kinase kinase kinase 1 (MAP3K1) is a target of miR-1a and simvastatin decreases MAP3K1 gene expression to induce skeletal muscle cell apoptosis to cause skeletal muscle injury by enhancement of miR-1a *in vitro* and *in vivo*. In perspectives, normalization of miR-1a or MAP3K1 dysregulation should be taken into consideration to prevent statin-induced myopathy clinically.

MATERIALS AND METHODS

An expanded Materials and Methods section is available in the Supplementary Materials.

Animals and experimental protocols

Apolipoprotein E knockout (*ApoE*$^{-/-}$) mice, 6-8 weeks of age, were purchased from Beijing Huafukang Animal Experimental Center (Beijing, China). The gender is mixed, and we tried to have 50% of each gender in each group. All animals were housed in temperature-controlled cages with a 12-hour light-dark cycle. Simvastatin were given to mice by gavage at a dose of 20 mg/kg/day for 8 weeks to induce skeletal injury as reported previously [15, 16]. This study was carried out in accordance with the ethical standards laid down in the 1964 Declaration of Helsinki and its later amendments. The animal protocol was reviewed and approved by the Animal Care and Use Committee of Shandong University Qilu Hospital.

Cell culture of skeletal muscle cells

As described previously [17], gastrocnemius muscle from 10 days old suckling mice (C57BL/6) was digested by collagenase II and trypsin at 37° C. After centrifugation, cells were suspended in DMEM medium containing 10% fetal bovine serum. Skeletal muscle satellite cells were isolated by using the difference of the adhesion speed with fibroblasts. 1. 2×10^6 cells were seeded in each well of 6-well plate. When the cell density reached 80-90%, medium was replaced with DMEM medium containing 2% horse serum, and the medium was changed every day. After 3 days, cells began to differentiate. After 5 days, 90% of satellite cells differentiated into mature skeletal muscle cells with the formation of myotubes and MHC expression (Supplementary Figure 1).

RNA extraction and real-time PCR

Extract total RNA from skeletal muscle cells or tissues using TRIzol Reagent according to manufacturer's instructions [18, 19].

Luciferase reporter assay

As described previously [7, 20], plasmid constructs (MAP3K1-UTR or MT-MAP3K1-UTR) were co-transfected in HEK293 cells with the pCMV β-gal plasmid and 50 nM each of chemically synthesized miR-1a or negative control oligonucleotides by using lipofectamine 2000. Cells were harvested 48 hours after transfection, and luciferase and β-galactosidase activities were measured.

Determination of exercise capacity

The exercise capacity was determined using forelimb grip strength test, hanging grid test, and exhaustive running test as previously reported [16].

Statistical analysis

Data are reported as mean ± SEM. A one-way ANOVA followed by Bonferroni correction was used for multiple comparisons. Two-sided *P*-value <0.05 was considered as significant.

RESULTS

Statin increases the expression of miR-1a in skeletal muscle cells

We firstly investigated the effects of statin in miR-1a expression in cultured skeletal muscle cells. Cultured skeletal muscle cells (originally differentiated from

gastrocnemius skeletal muscle satellite cells isolated from suckling mice) were treated with varying concentrations of simvastatin from 1 to 24 h. The expressional level of miR-1a in skeletal muscle cells gradually increased beginning 6 h after incubation with 5 μM of simvastatin and continued to increase at 12h and 24h (Figure 1A). Next, we examined the dose-dependent effects of simvastatin on miR-1a expression (Figure 1B). Simvastatin increased miR-1a expression at a concentration of 0.5 μM. Increasing concentrations of simvastatin (1-5 μM) further enhanced miR-1a expression. These data indicate that statin induces excessive expression of miR-1a in skeletal muscle cells.

Statin induces skeletal muscle cell apoptosis through miR-1a

Previous studies had reported that miR-1a mediates cell apoptosis [12, 13]. Thus, we examined the role of miR-1a in statin-induced cells apoptosis by transfecting miR-1a inhibitor or mimics into skeletal muscle cells, which was specially changed miR-1a expression (Supplementary Figure 2A), indicating the on-target effect. Protein levels of pro-/cleaved-caspase3, 7, 9, bcl-2, and bax, were assayed by western blot to represent cell apoptosis. As shown in Figure 2A–2C, simvastatin increased the ratio of cleaved-caspase3, 7, 9 to pro-caspase3, 7, 9 and decreased the ratio of bcl-2 to bax. As expected, these effects of statin were inhibited by miR-1a inhibitor but exacerbated by miR-1a mimics.

Cell apoptosis was assayed by using TUNEL and flow cytometry methods. As presented in Figure 2D, 2E, similar to apoptosis-related proteins, statin significantly induced cell apoptosis of skeletal muscle cells, which were bypassed by miR-1a inhibitor. Taking these data together, it suggests that satin induces skeletal muscle cell apoptosis through miR-1a activation. Cell apoptosis was further confirmed by measuring cell viability using CCK8 method as described previously [21]. Statin significantly decreased the number of viable cells in cells transfected with miR-1a inhibitor negative control, but not in cells transfected with miR-1a inhibitor (Supplementary Figure 2B).

MAP3K1 is a target gene of miR-1a

Computational target-scan analysis (Figure 3A) showed that miR-1a potentially binds to the highly conserved target site (1589-1595, 5′-ACAUUCC-3′) in the 3′-UTR of MAP3K1 mRNA. This suggested that miR-1a may inhibit the expression of MAP3K1 through post-transcriptional regulation. To examine if miR-1a can repress MAP3K1 gene expression through direct 3′-UTR interaction, we cloned MAP3K1 3′-UTR luciferase reporter plasmid and performed reporter analysis in HEK293 cells. As shown in Figure 3B, co-transfection of miR-1a with plasmid of MAP3K1 3′-UTR reporter resulted in a significant inhibition of luciferase activity. Further, miR-1a failed to suppress the activity of MAP3K1 3′-UTR reporter with a mutated miR-1a seed sequence. These data indicated that MAP3K1 mRNA is a direct target of miR-1a. Moreover, we measured the effects of overexpression of miR-1a on MAP3K1 mRNA using real-time PCR (Figure 3C) and protein using Western blot (Figure 3D).

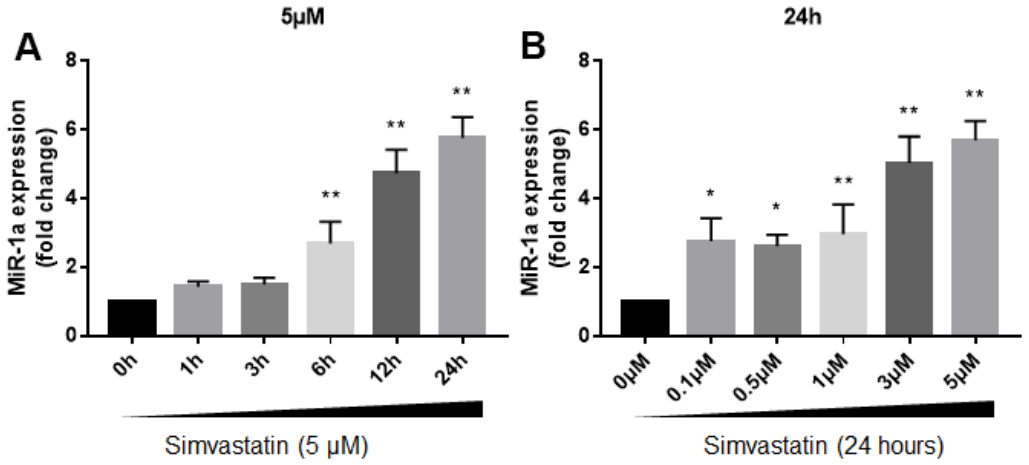

Figure 1. Statin induces excessive expression of miR-1a in skeletal muscle cells. (**A**) Cultured skeletal muscle cells were treated with simvastatin (5 μM) as indicated time points. The expressions of miR-1a was assayed using quantitative real-time PCR. N = 5 per group. $^{**}P <$ 0.01 vs. control group (0 h). (**B**) Cultured skeletal muscle cells were treated with simvastatin (24 hours) as indicated concentration points. The expressions of miR-1a was assayed using quantitative real-time PCR. N = 5 per group. $^{*}P < 0.05$ or $^{**}P < 0.01$ vs. control group (0 μM). A one-way ANOVA followed by Tukey *post-hoc* tests was used to determine *P* value in (**A**, **B**).

Overexpression of miR-1a significantly decreased both mRNA and protein levels of MAP3K1, compared to negative control, further supporting the notion that miR-1a functions as a regulator of MAP3K1 gene expression.

Statin decreases the protein expression of MAP3K1 in cells

Knowing MAP3K1 is a target gene of miR-1a and statin increases miR-1a expression in skeletal muscle cells, we thought that statin reduces MAP3K1 levels in skeletal muscle cells. As expected, statin decreased the protein expression of MAP3K1 in cultured skeletal muscle cells, also in a dose or time dependent manner (Supplementary Figure 3A, 3B).

Statin induces skeletal muscle cell apoptosis via MAP3K1 deficiency

MAP3K1 is a key factor to control cell apoptosis [22]. Therefore, we determined whether MAP3K1 plays roles in statin-induced skeletal muscle cell apoptosis. As shown in Figure 4A–4D, overexpression of MAP3K1 dramatically inhibited the effects of statin on caspase3, 7, 9, bcl-2, and bax in skeletal muscle cells. Consistently, overexpression of MAP3K1 also abrogated statin-induced cell apoptosis of skeletal muscle cells as determined by flow cytometry (Figure 4E). As shown by the result of CCK8, overexpression of MAP3K1 increased the number of viable cells, which was excessively reduced by statin stimulation (Supplementary Figure 3D).

Statin induces cell apoptosis through the miR-1a-MAP3K1 pathway

Since either miR-1a inhibition or MAP3K1 overexpression prevents statin-induced skeletal muscle cell apoptosis, we thought that MAP3K1 may function as a downstream mediator of miR-1a in regulation of cell apoptosis. To this viewpoint, we co-transfected cells with miR-1a inhibitor and MAP3K1 siRNA. As

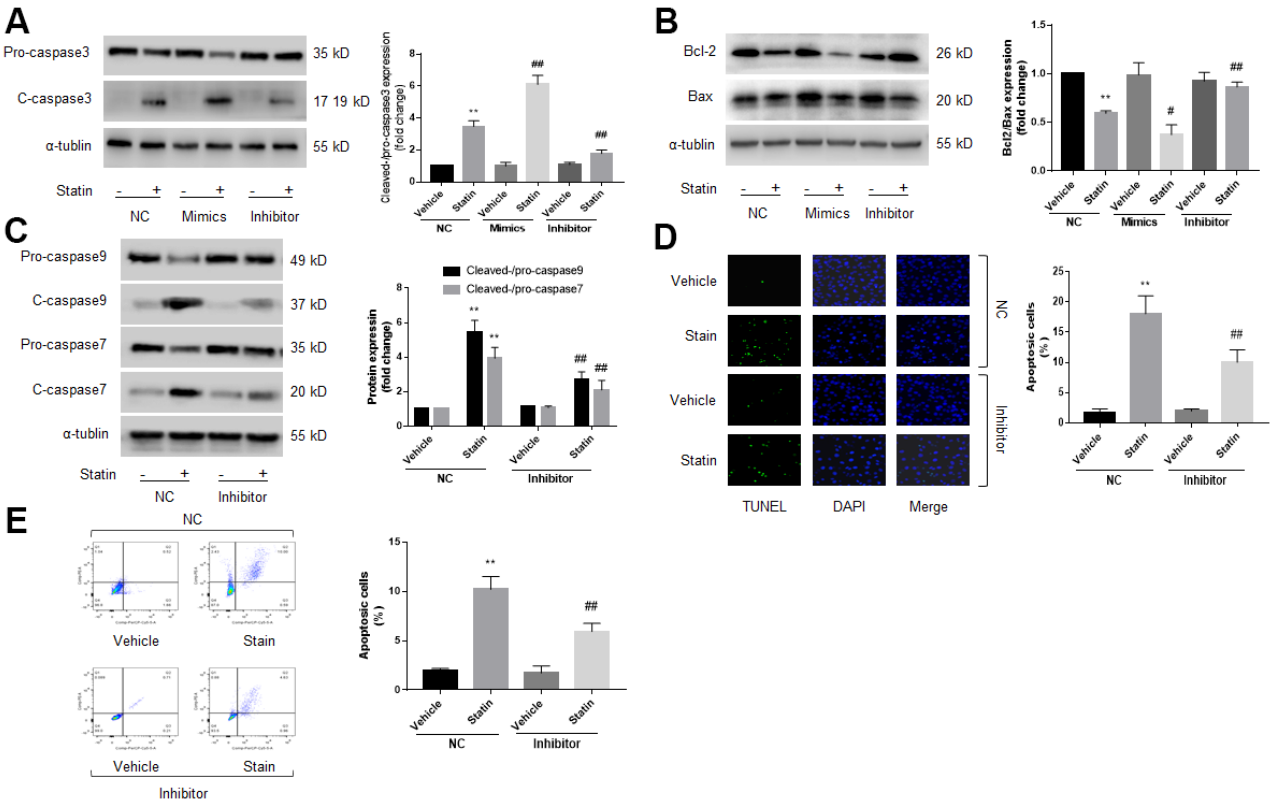

Figure 2. Statin induces cell apoptosis via upregulation of miR-1a in skeletal muscle cells. (**A**–**C**) Cultured skeletal muscle cells were transfected with miR-1a mimics and inhibitors for 48 hours followed by statin treatment for 24 hours. Cells were subjected to detect the protein levels of pro-/cleaved-caspase3 in (**A**) bcl-2 and bax in (**B**) and pro-/cleaved-caspase7, 9 in (**C**) by western blot. N is 5 in each group. $^{**}P$<0.01 vs. NC alone. $^{\#}P$<0.05 or $^{\#\#}P$<0.01 vs. statin alone. (**D**, **E**) Cultured skeletal muscle cells were transfected with miR-1a inhibitor for 48 hours followed by statin treatment for 24 hours. Cell apoptosis was determined by TUNEL method in (**D**) and flow cytometry in (**E**). N is 5 in each group. $^{**}P$<0.01 vs. NC alone. $^{\#\#}P$<0.01 vs. statin alone. A one-way ANOVA followed by Tukey *post-hoc* tests was used to determine *P* value in (**A**–**E**).

shown in Figure 5A–5C, though statin-induced alterations of caspase3, 7, 9, bcl-2 and bax proteins were abolished by miR-1a inhibitor, miR-1a inhibitor had no effects in statin-treated cells if transfected with MAP3K1 siRNA. Both TUNEL assay and flow cytometry indicated that the inhibitory effects of miR-1a inhibitor on statin-induced apoptosis were completely prevented by MAP3K1 siRNA (Figure 5D, 5E). CCK8 showed consistent result (Supplementary Figure 4A, 4B). Together, these data suggest that statin induces cell apoptosis through the miR-1a-MAP3K1 pathway in skeletal muscle cells.

Inhibition of miR-1a prevents statin-induced muscle injury in mice

We next investigated the roles of miR-1a in statin-induced skeletal injury *in vivo*. *ApoE*$^{-/-}$ mice, with the background of natural hyperlipidemia [23, 24], was selected in this study. The protocol for animal experiment was shown in Figure 6A. HE staining of gastrocnemius muscle revealed marked variations in skeletal muscle fibre size and arrangement, as well as decreased fibre cross-sectional area (CSA) in statin administration group. While, lentivirus-mediated miR-1a inhibition abrogated statin-induced fibre disorganization and CSA decrease (Figure 6B, 6C). Also, the indexes of muscle damage including CK and LDH, were normalized by miR-1a inhibition in statin-treated mice, compared to mice infected with lentivirus vector (Figure 7A, 7B). These data imply that inhibition of miR-1a improves statin-induced muscle damage *in vivo*.

miR-1a inhibition improves statin-impaired exercise capacity in mice

Statin-induced skeletal injury was further assessed using exercise capacity by calculating forelimb grip strength test, hanging grid test, and exhaustive running test as reported previously [16]. As presented in Figure 7C–7F, statin administration reduced the exercise capacity in *ApoE*$^{-/-}$ mice infected with lentivirus vector, but not in *ApoE*$^{-/-}$ mice infected lentivirus expressing miR-1a inhibitor, further supporting that statin induces skeletal myopathy through induction of miR-1a in mice.

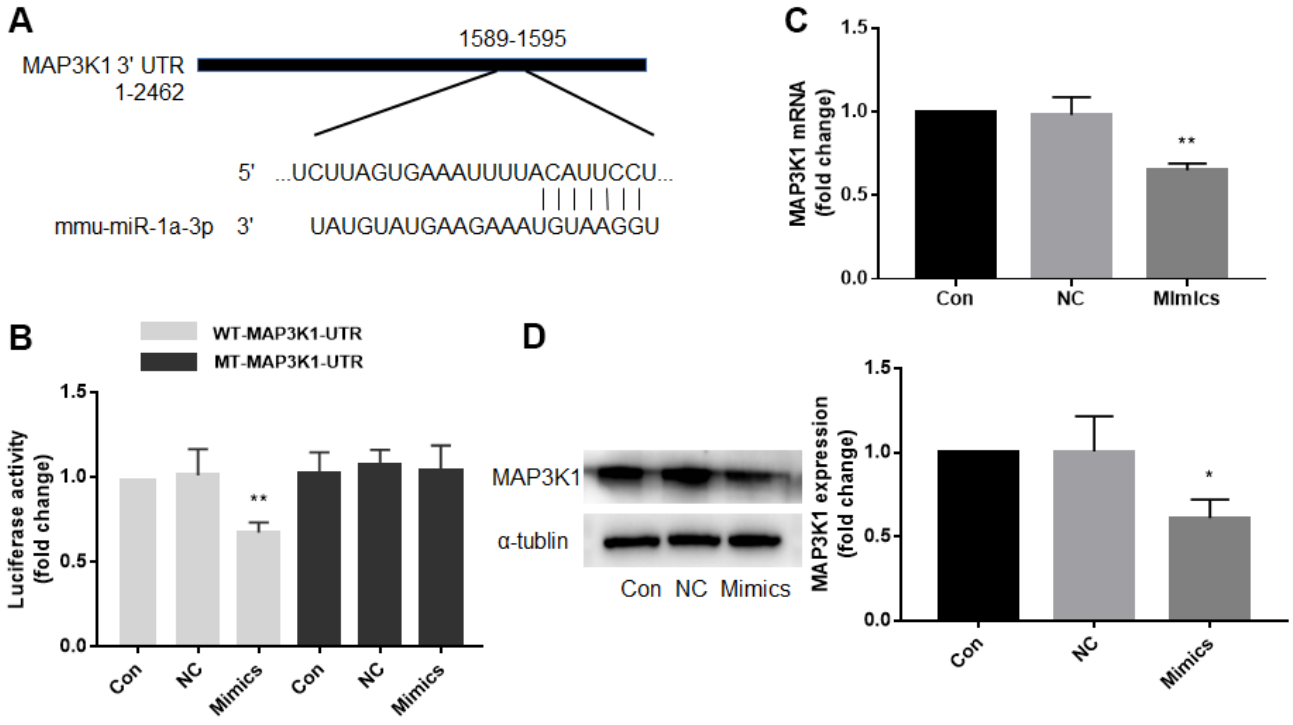

Figure 3. Mitogen-activated protein kinase kinase kinase 1 (MAP3K1) is a target gene of miR-1a. (**A**) Computational target-scan analysis showed that miR-1a is able to bind the highly conserved target site (1589-1595, 5′-ACAUUCC-3′) in the 3′-UTR of MAP3K1 mRNA. (**B**) Plasmid of luciferase reporter construction containing 3′-UTR of MAP3K1 mRNA (WT-MAP3K1-UTR) or mutant of MAP3K1-UTR (MT-MAP3K1-UTR) was co-transfected with miR-1a negative control (NC) or mimics in HEK293 cells. The luciferase activities in total cell lysates were assayed. N is 5 in each group. $^{**}P$<0.01 vs. NC. (**C**, **D**) Cultured skeletal muscle cells were transfected with miR-1a NC and mimics for 48 hours. The mRNA level of MAP3K1 in (**C**) and protein level in (**D**) were analyzed using real-time PCR and western blot, respectively. N is 5 in each group. $^{*}P < 0.05$ or $^{**}P < 0.01$ vs. NC. A one-way ANOVA followed by Tukey *post-hoc* tests was used to determine *P* value in (**B**–**D**).

Inhibition of miR-1a prevents statin-induced skeletal muscle cell apoptosis in *ApoE*$^{-/-}$ mice

Finally, we examined the effects of miR-1a inhibition on statin-induced cell apoptosis *in vivo*. As indicated in Supplementary Figure 5A, 5B, simvastatin upregulated miR-1a gene expression but downregulated MAP3K1 protein expression, which were reversed by lentivirus-mediated gene silence of miR-1a. Further, statin increased the ratio of cleaved-caspase3, 7, 9 to pro- caspase3, 7, 9, decreased the ratio of bcl-2 to bax (Figure 8A–8C), increased the expression of cleaved-caspase3 (Figure 8D) and induced cells apoptosis in gastrocnemius (Figure 8E). Importantly, all of these phenotypes induced by simvastatin were prevented by miR-1a downregulation.

Body weight, food intake, and serum cholesterol content of mice during the experimental cycle

Relevant data are presented in Supplementary Tables 1–3.

DISCUSSION

In this study, we firstly demonstrated that statin induced excessive expression of miR-1a to cause skeletal injury *in vivo*. Mechanically, miR-1a represses MAP3K1 gene expression by targeting of the 3'-UTR of mRNA to promote skeletal muscle cell apoptosis. To the best of our knowledge, this study is firstly to report that statin via induction of miR-1a decreases MAP3K1 to induce skeletal myopathy.

The major discovery of the study is that MAP3K1 is a target of miR-1a in skeletal muscle cells. It has been reported that miR-1a plays an important role in multiple cellular functions, such as differentiation of chondrocytes and skeletal muscle satellite cells [25, 26], maintaining normal rhythm of cardiomyocytes [27], and reinforcing the striated muscle phenotype [28]. In particular, miR-1a regulates the apoptotic process of many cells, such as prostate cancer cells [29], nerve cells [30], and cardiomyocytes [31]. In this study, we

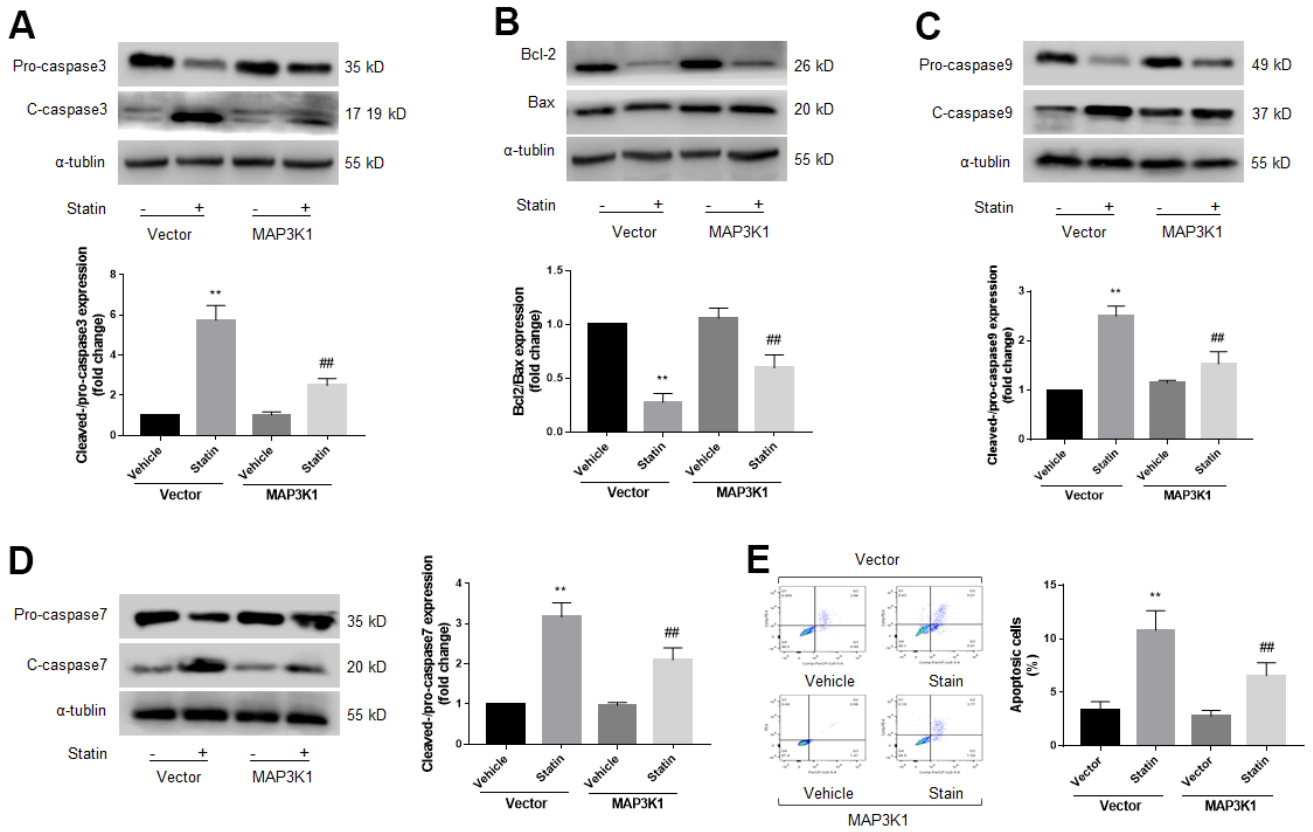

Figure 4. Statin induces cell apoptosis of skeletal muscle cells via downregulation of MAP3K1. Cultured skeletal muscle cells were transfected with plasmids MAP3K1 cDNA for 48 hours followed by statin treatment for 24 hours. Cells were subjected to detect the protein levels of pro-/cleaved-caspase3 in (**A**) bcl-2 and bax in (**B**) pro-/cleaved-caspase9 in (**C**) and pro-/cleaved-caspase7 in (**D**) by western blot. Cell apoptosis was determined by flow cytometry in (**E**). N is 5 in each group. $^{**}P$<0.01 vs. vector alone. $^{\#\#}P$<0.01 vs. statin plus vector. A one-way ANOVA followed by Tukey *post-hoc* tests was used to determine *P* value in (**A**–**E**).

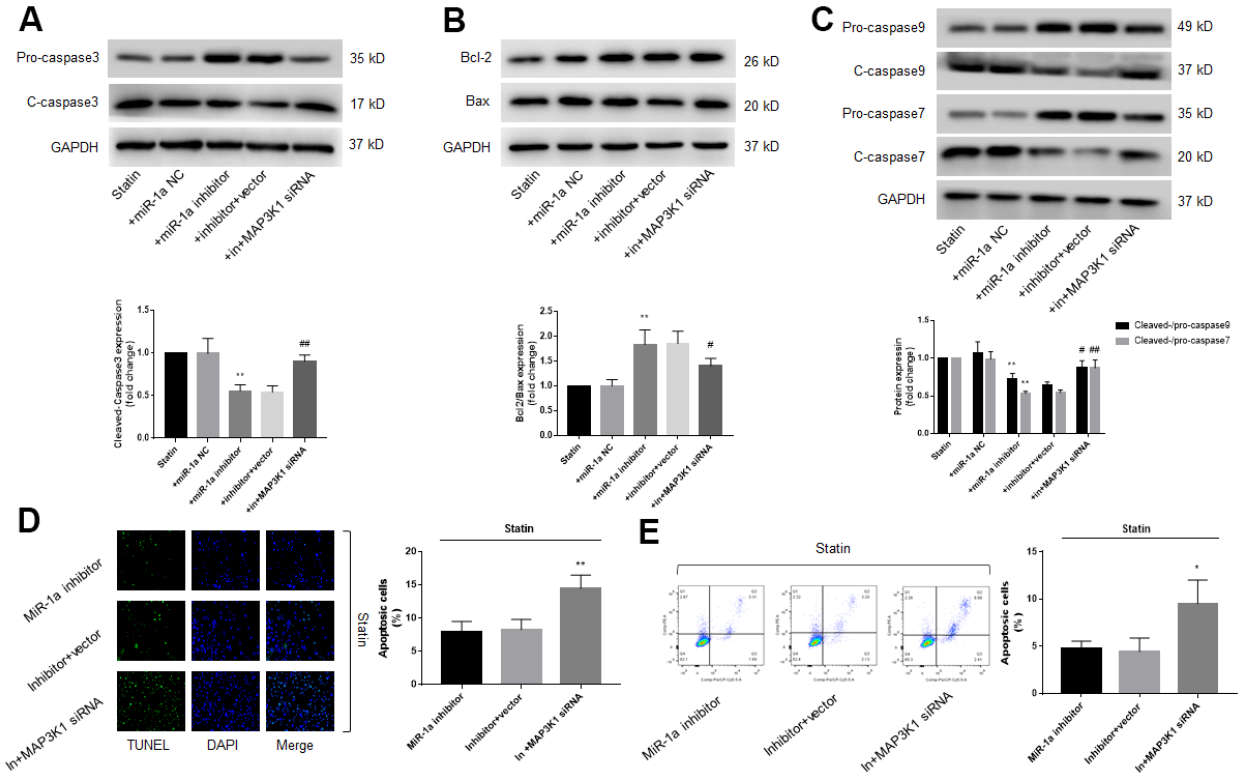

Figure 5. The miR-1a-MAP3K1 pathway mediates statin-induced cell apoptosis in skeletal muscle cells. Cultured skeletal muscle cells were transfected with miR-1a inhibitor and/or MAP3K1 siRNA for 48 hours followed by statin treatment for 24 hours. (**A**–**C**) Cells were subjected to detect the protein levels of pro-/cleaved-caspase3 in (**A**) bcl-2 and bax in (**B**) and pro-/cleaved-caspase7, 9 in (**C**) by western blot. N is 5 in each group. $^{**}P$<0.01 vs. statin alone. $^{\#}P$<0.05 or $^{\#\#}P$<0.01 vs. statin plus miR-1a inhibitor. (**D**, **E**) Cell apoptosis was determined by TUNEL in (**D**) and flow cytometry in (**E**). $^{*}P < 0.05$ or $^{**}P < 0.01$ vs. statin plus miR-1a inhibitor. A one-way ANOVA followed by Tukey *post-hoc* tests was used to determine *P* value in (**A**–**E**).

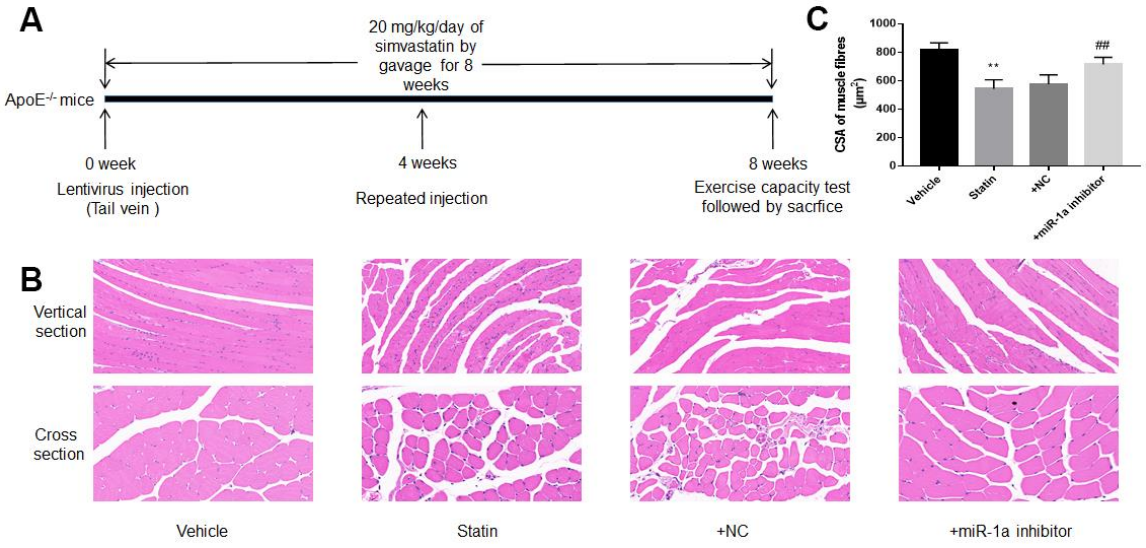

Figure 6. Downregulation of miR-1a prevents statin-induced morphological deterioration of gastrocnemius in *ApoE*$^{-/-}$ mice. (**A**) The protocol for animal experiments was shown. (**B**) The morphology of gastrocnemius muscle was observed by HE staining. (**C**) Quantitative analysis of fibre cross-sectional area (CSA) in gastrocnemius muscle from mice was performed. N is 10-15 in each group. $^{**}P <$ 0.01 vs. vehicle group. $^{\#\#}P$<0.01 vs. statin alone. A one-way ANOVA followed by Tukey *post-hoc* tests was used to determine *P* value in (**C**).

further exploited that MAP3K1 is a novel target of miR-1a in skeletal muscle cells. This was demonstrated by the following evidences: (1) miR-1a target site is found to be located in the 3'-UTR of MAP3K1 mRNA as indicated "5'-ACAUUCC-3'"; (2) Transfection of miR-1a decreased luciferase reporter activity in plasmid of MAP3K1 3′-UTR, but not in plasmid of MAP3K1 3′-UTR with the mutant of miR-1a target site; (3) MAP3K1 as a target of miR-1a was further supported in both cultured cells and *ApoE*$^{-/-}$ mice, in which loss-function of miR-1a increased MAP3K1 gene expression. This discovery not only uncovers a novel mechanism of MAP3K1 posttranslational gene regulation, but also broadens the biological functions of miR-1a.

In the present study, we further illustrated that statin induces miR-1a to cause skeletal muscle cell apoptosis and injury *in vitro* and *in vivo*. We transfected skeletal muscle cells with miR-1a mimics and inhibitor, respectively. From the results of apoptosis-related proteins, TUNEL assay and flow cytometry, it can be affirmatory that statin increases the apoptotic level of skeletal muscle cells, while the apoptotic level is further increased after overexpression of miR-1a, and is suppressed after inhibition of miR-1a. CCK8 results showed that statin reduced the number of viable cells, while inhibition of miR-1a increased the viable cell number, which indicated decreased cytotoxicity. *In vivo*, lentivirus-mediated inhibition of miR-1a similarly suppressed statin induced apoptosis in skeletal muscle, as indicated by apoptosis related-proteins and TUNEL.

MAP3K1 has both anti- and pro-apoptotic functions depending on the cell type and stimulus [22]. In order to determine whether MAP3K1 has anti-apoptotic or pro-apoptotic effects on statin-induced skeletal muscle cell injury, we overexpressed MAP3K1 in statin-treated skeletal muscle cells. According to the results reflected by western blot, flow cytometry and TUNEL assay, overexpression of MAP3K1 can improve the cell apoptosis. By inhibiting the expression of MAP3K1 through siRNA, the anti-apoptotic effect of miR-1a inhibition was prevented. This indicates that MAP3K1 of skeletal muscle cells has anti-apoptotic effect under the stimulation of statins. The miR-1a-MAP3K1 pathway, which is firstly reported by us, is involved in statin-induced skeletal muscle toxicity.

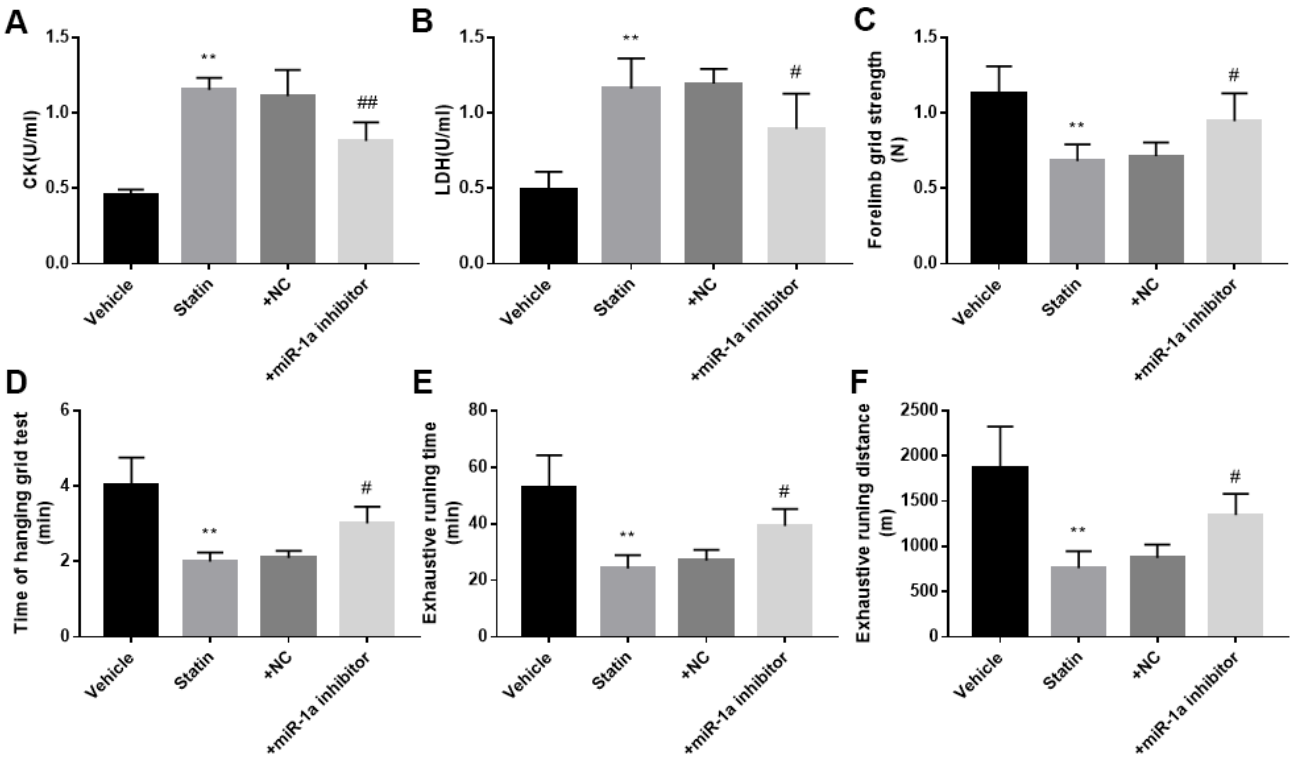

Figure 7. Inhibition of miR-1a improves the exercise ability in mice treated with statin. The protocol for animal experiments was shown in Figure 6A. (**A**, **B**): The levels of creatine kinase (CK) and lactate dehydrogenase (LDH) in plasma from mice were assayed. (**C**–**F**) The exercise capacity was determined, and the forelimb grip strength in (**C**) hanging grid time in (**D**) exhaustive running time in (**E**) and distance of exhaustive running in (**F**) were calculated. N is 10-15 in each group. $^{**}P < 0.01$ vs. PBS group. $^{\#}P<0.05$ or $^{\#\#}P<0.01$ vs. statin alone. A one-way ANOVA followed by Tukey *post-hoc* tests was used to determine *P* value in (**A**–**F**).

Traditionally, statin has been reported to prevent cardiovascular diseases [32], but produces some side effects including skeletal dysfunctions. Multiple mechanisms have been suggested contributing to statin toxicity, such as reduced sarcolemma or T-tubule cholesterol [33], reduction in CoQ10 [34], activation of the phosphoinositide 3 kinase pathway [2], and impaired mitochondrial function [35]. In this study, our data indicate that the detrimental effects of statin on skeletal function depend on miR-1a because lentivirus-mediated inhibition of miR-1a prevented statin-reduced exercise capacity in *ApoE*$^{-/-}$ mice. Thus, we reveal a uniform miR-1a-mediated mechanism of statin on impairing skeletal functions. Of note, how statin induces miR-1a expression in skeletal cells needs further investigations.

There are many miRs and proteins related to myoblast proliferation and differentiation, such as miR-133a, miR-206, SRF, mTOR/MyoD and MEF2, and we detected the expression of these miRs and proteins under statin stimulation. The results showed that, compared with the control group, the expression of miR-133a, SRF increased, while the expression of miR-206, mTOR, MEF2, MyoD did not change significantly (Supplementary Figure 7). The relationship between miR-133a, SRF and statin-induced muscle injury requires further investigation. We also detected other death pathways in skeletal muscle cells, and the data confirmed that under statin stimulation, skeletal muscle cells had increased necroptosis without significant changes in pyroptosis (Supplementary Figure 8).

A recent report suggests that statin-induced myopathy is associated with the inhibition of mitochondrial complex III [36]. Since mitochondrion has a critical role in apoptosis, this inspired our imagination: Statins-induced mitochondrial complex III inhibition may be related to excessive expression of miR-1a. In the future, we will test this hypothesis.

Nevertheless, our study has several shortcomings: i) Since our study animals were 6-8 weeks old and we did

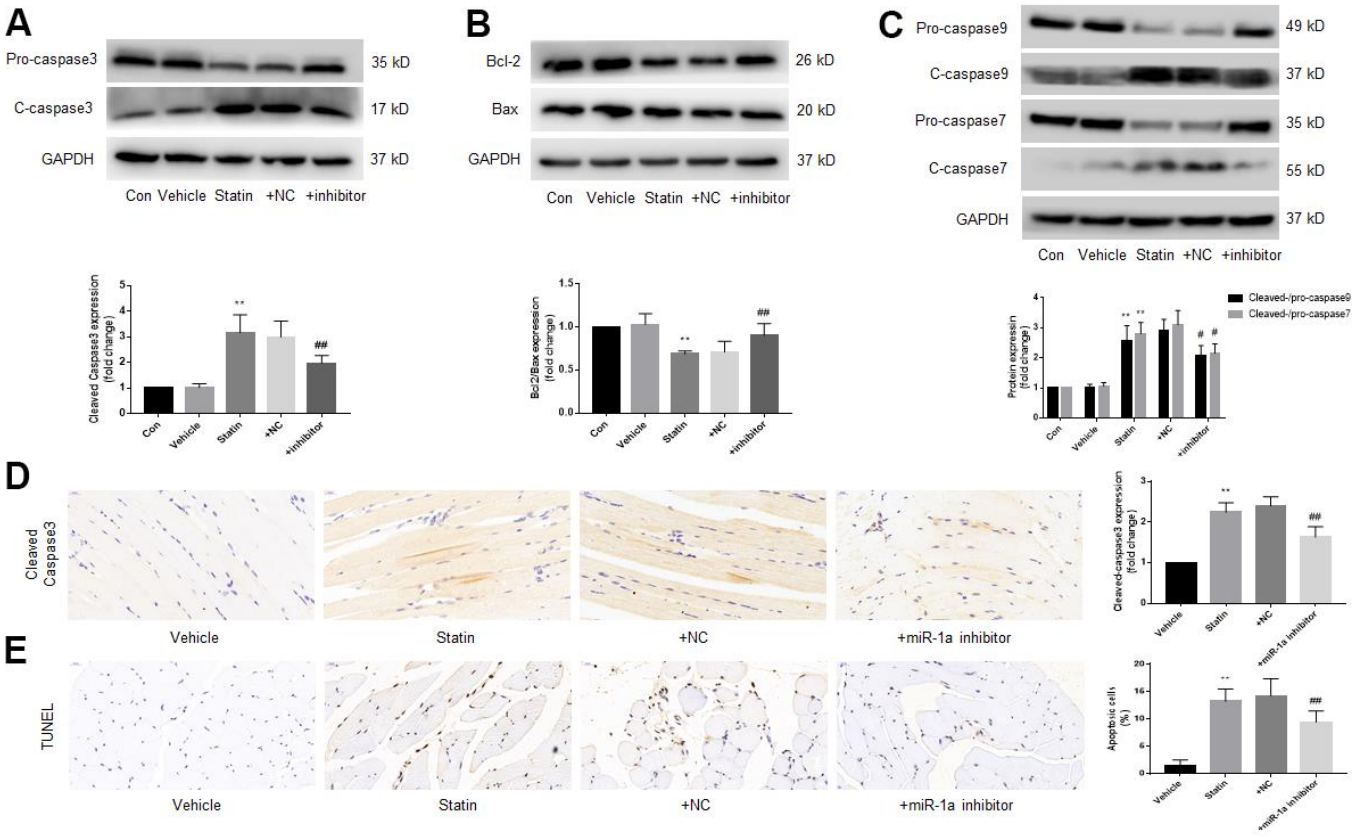

Figure 8. Downregulation of miR-1a expression inhibits the apoptosis of gastrocnemius muscle cells induced by statin *in vivo*. The protocol for animal experiments was shown in Figure 6A. (**A**–**C**) Expressional levels of pro-/cleaved-caspase3, 7, 9, bcl-2 and bax in gastrocnemius were assayed by western blot. (**D**) Cleaved-caspase3 in gastrocnemius were assayed by IHC. (**E**) Cell apoptosis in gastrocnemius was determined by TUNEL method. N is 10-15 in each group. $^{**}P < 0.01$ vs. vehicle group. $^{\#}P<0.05$ or $^{\#\#}P<0.01$ vs. statin alone. A one-way ANOVA followed by Tukey *post-hoc* tests was used to determine *P* value in (**A**–**E**).

not study aged mice. Previous studies have shown that age is an important factor affecting statin side effects [37]. So, we speculated that the protective effect on statin muscle injury exerted by miR-1a inhibition would be different in aged mice. The effect of age on the protective effect of miR-1a inhibitor would be our next research direction. ii) Simvastatin is a lipophilic statin and most of our studies adopted it. We only have a small number of studies on hydrophilic statin (pravastatin) (Supplementary Figure 6). The results showed that pravastatin also significantly increased the expression of miR-1a, and inhibition of miR-1a similarly reduced statin-induced apoptosis in skeletal muscle cells. However, concluding that 'statins cause skeletal muscle toxicity by increasing miR-1a' may still be somewhat powerless.

ApoE-/- and Ldlr-/- mice are the two most frequently used murine models for hyperlipidemia. According to some reports, experiments on these two models may present different results, and additionally different gender may also affect the experimental results. So, in the next step, we will use Ldlr-/- mice to verify if our results are reproducible and will also present the results of experiments in different genders separately.

In summary, this study reveals a novel mechanism of statin to cause skeletal myopathy. As present in Supplementary Figure 9, statin increases miR-1a expression to decrease MAP3K1, resulting in cell apoptosis of skeletal muscle cells. In this way, statin causes skeletal injury in mice. Therefore, the current study will open some new avenues to investigate the roles of miR-1a in statin's side effects and also provide some insights to drug design for myopathy in that targeting miR-1a to improve the outcomes of medical intervention.

AUTHOR CONTRIBUTIONS

C.N.F. conceived the study, performed most experiments, and wrote the draft of the paper. J.W.S., Q.W.W., Z.P.S., W.W.B., T.G., and P.L. partially conducted some experiments. C.L. and B.D. helped to analyze the data and organize the manuscript. S.X.W. revised this paper and supervised the study.

CONFLICTS OF INTEREST

The authors declare that they have no conflicts of interest.

FUNDING

This project was supported by National Natural Science Foundations of China (82070382, 82000360, 81970693, 81874312, 81870283, and 81770493) and the Key Research and Development Program of Shandong Province (2019GSF108070 and ZR2020MH040). S.X.W. is a distinguished professor of Henan province, a recipient of Zhong-Yuan-Qian-Ren Program of Henan province (194200510005), a Tai-Hang Professional Scholarship of Xinxiang Medical University (505067), an exceptional young scholar of Shandong University, and an adjunct Lan-Yue Professional Scholar of Hubei University of Science and Technology (2020TNB01). B.D. was sponsored by the Tai-Shan scholars program (No: ts20190979).

REFERENCES

1. Kozarov E, Padro T, Badimon L. View of statins as antimicrobials in cardiovascular risk modification. Cardiovasc Res. 2014; 102:362–74. https://doi.org/10.1093/cvr/cvu058 PMID:24623278

2. Thompson PD, Panza G, Zaleski A, Taylor B. Statin-Associated Side Effects. J Am Coll Cardiol. 2016; 67:2395–410. https://doi.org/10.1016/j.jacc.2016.02.071 PMID:27199064

3. Ma H, Liang WJ, Shan MR, Wang XQ, Zhou SN, Chen Y, Guo T, Li P, Yu HY, Liu C, Yin YL, Wang YL, Dong B, et al. Pravastatin activates activator protein 2 alpha to augment the angiotensin II-induced abdominal aortic aneurysms. Oncotarget. 2017; 8:14294–305. https://doi.org/10.18632/oncotarget.15104 PMID:28179583

4. Singh F, Zoll J, Duthaler U, Charles AL, Panajatovic MV, Laverny G, McWilliams TG, Metzger D, Geny B, Krähenbühl S, Bouitbir J. PGC-1β modulates statin-associated myotoxicity in mice. Arch Toxicol. 2019; 93:487–504. https://doi.org/10.1007/s00204-018-2369-7 PMID:30511338

5. Bouitbir J, Singh F, Charles AL, Schlagowski AI, Bonifacio A, Echaniz-Laguna A, Geny B, Krähenbühl S, Zoll J. Statins trigger mitochondrial reactive oxygen species-induced apoptosis in glycolytic skeletal muscle. Antioxid Redox Signal. 2016; 24:84–98. https://doi.org/10.1089/ars.2014.6190 PMID:26414931

6. Rhoades MW, Reinhart BJ, Lim LP, Burge CB, Bartel B, Bartel DP. Prediction of plant microRNA targets. Cell. 2002; 110:513–20. https://doi.org/10.1016/S0092-8674(02)00863-2Z PMID:12202040

7. Li P, Yin YL, Guo T, Sun XY, Ma H, Zhu ML, Zhao FR, Xu P, Chen Y, Wan GR, Jiang F, Peng QS, Liu C, et al. Inhibition of aberrant MicroRNA-133a expression in

endothelial cells by statin prevents endothelial dysfunction by targeting GTP cyclohydrolase 1 *in vivo*. Circulation. 2016; 134:1752–65. https://doi.org/10.1161/CIRCULATIONAHA.116.017949 PMID:27765794

8. Wang F, Ma H, Liang WJ, Yang JJ, Wang XQ, Shan MR, Chen Y, Jia M, Yin YL, Sun XY, Zhang JN, Peng QS, Chen YG, et al. Lovastatin upregulates microRNA-29b to reduce oxidative stress in rats with multiple cardiovascular risk factors. Oncotarget. 2017; 8:9021–34. https://doi.org/10.18632/oncotarget.14462 PMID:28061433

9. Calvano J, Achanzar W, Murphy B, DiPiero J, Hixson C, Parrula C, Burr H, Mangipudy R, Tirmenstein M. Evaluation of microRNAs-208 and 133a/b as differential biomarkers of acute cardiac and skeletal muscle toxicity in rats. Toxicol Appl Pharmacol. 2016; 312:53–60. https://doi.org/10.1016/j.taap.2015.11.015 PMID:26627004

10. Xiao J, Pan Y, Li XH, Yang XY, Feng YL, Tan HH, Jiang L, Feng J, Yu XY. Cardiac progenitor cell-derived exosomes prevent cardiomyocytes apoptosis through exosomal miR-21 by targeting PDCD4. Cell Death Dis. 2016; 7:e2277. https://doi.org/10.1038/cddis.2016.181 PMID:27336721

11. Wang JX, Zhang XJ, Li Q, Wang K, Wang Y, Jiao JQ, Feng C, Teng S, Zhou LY, Gong Y, Zhou ZX, Liu J, Wang JL, Li PF. MicroRNA-103/107 regulate programmed necrosis and myocardial ischemia/ reperfusion injury through targeting FADD. Circ Res. 2015; 117:352–63. https://doi.org/10.1161/CIRCRESAHA.117.305781 PMID:26038570

12. Liu R, Li J, Lai Y, Liao Y, Liu R, Qiu W. Hsa-miR-1 suppresses breast cancer development by down-regulating K-ras and long non-coding RNA MALAT1. Int J Biol Macromol. 2015; 81:491–97. https://doi.org/10.1016/j.ijbiomac.2015.08.016 PMID:26275461

13. Xu Y, Zheng M, Merritt RE, Shrager JB, Wakelee HA, Kratzke RA, Hoang CD. miR-1 induces growth arrest and apoptosis in malignant mesothelioma. Chest. 2013; 144:1632–43. https://doi.org/10.1378/chest.12-2770 PMID:23828229

14. Horak M, Novak J, Bienertova-Vasku J. Muscle-specific microRNAs in skeletal muscle development. Dev Biol. 2016; 410:1–13. https://doi.org/10.1016/j.ydbio.2015.12.013 PMID:26708096

15. Penson PE, Mancini GB, Toth PP, Martin SS, Watts GF, Sahebkar A, Mikhailidis DP, Banach M, and Lipid and Blood Pressure Meta-Analysis Collaboration (LBPMC) Group & International Lipid Expert Panel (ILEP). Introducing the 'Drucebo' effect in statin therapy: a systematic review of studies comparing reported rates of statin-associated muscle symptoms, under blinded and open-label conditions. J Cachexia Sarcopenia Muscle. 2018; 9:1023–33. https://doi.org/10.1002/jcsm.12344 PMID:30311434

16. Song M, Chen FF, Li YH, Zhang L, Wang F, Qin RR, Wang ZH, Zhong M, Tang MX, Zhang W, Han L. Trimetazidine restores the positive adaptation to exercise training by mitigating statin-induced skeletal muscle injury. J Cachexia Sarcopenia Muscle. 2018; 9:106–18. https://doi.org/10.1002/jcsm.12250 PMID:29152896

17. Musarò A, Carosio S. Isolation and culture of satellite cells from mouse skeletal muscle. Methods Mol Biol. 2017; 1553:155–67. https://doi.org/10.1007/978-1-4939-6756-8_12 PMID:28229414

18. Bai YP, Zhang JX, Sun Q, Zhou JP, Luo JM, He LF, Lin XC, Zhu LP, Wu WZ, Wang ZY, Zhang GG. Induction of microRNA-199 by nitric oxide in endothelial cells is required for nitrovasodilator resistance via targeting of prostaglandin I2 synthase. Circulation. 2018; 138:397–411. https://doi.org/10.1161/CIRCULATIONAHA.117.029206 PMID:29431644

19. Liang WJ, Zhou SN, Shan MR, Wang XQ, Zhang M, Chen Y, Zhang Y, Wang SX, Guo T. AMPKα inactivation destabilizes atherosclerotic plaque in streptozotocin-induced diabetic mice through AP-2α/miRNA-124 axis. J Mol Med (Berl). 2018; 96:403–12. https://doi.org/10.1007/s00109-018-1627-8 PMID:29502204

20. Zhou SN, Lu JX, Wang XQ, Shan MR, Miao Z, Pan GP, Jian X, Li P, Ping S, Pang XY, Bai YP, Liu C, Wang SX. S-nitrosylation of prostacyclin synthase instigates nitrate cross-tolerance *in vivo*. Clin Pharmacol Ther. 2019; 105:201–09. https://doi.org/10.1002/cpt.1094 PMID:29672839

21. Shan MR, Zhou SN, Fu CN, Song JW, Wang XQ, Bai WW, Li P, Song P, Zhu ML, Ma ZM, Liu Z, Xu J, Dong B, et al. Vitamin B6 inhibits macrophage activation to prevent lipopolysaccharide-induced acute pneumonia in mice. J Cell Mol Med. 2020; 24:3139–48. https://doi.org/10.1111/jcmm.14983 PMID:31970902

22. Pham TT, Angus SP, Johnson GL. MAP3K1: genomic alterations in cancer and function in promoting cell survival or apoptosis. Genes Cancer. 2013; 4:419–26.

https://doi.org/10.1177/1947601913513950
PMID:24386504

23. Yang JJ, Li P, Wang F, Liang WJ, Ma H, Chen Y, Ma ZM, Li QZ, Peng QS, Zhang Y, Wang SX. Activation of activator protein 2 alpha by aspirin alleviates atherosclerotic plaque growth and instability *in vivo*. Oncotarget. 2016; 7:52729–39. https://doi.org/10.18632/oncotarget.10400 PMID:27391154

24. Wang S, Zhang C, Zhang M, Liang B, Zhu H, Lee J, Viollet B, Xia L, Zhang Y, Zou MH. Activation of AMP-activated protein kinase α2 by nicotine instigates formation of abdominal aortic aneurysms in mice *in vivo*. Nat Med. 2012; 18:902–10. https://doi.org/10.1038/nm.2711 PMID:22561688

25. Koning M, Werker PM, van der Schaft DW, Bank RA, Harmsen MC. MicroRNA-1 and microRNA-206 improve differentiation potential of human satellite cells: a novel approach for tissue engineering of skeletal muscle. Tissue Eng Part A. 2012; 18:889–98. https://doi.org/10.1089/ten.tea.2011.0191 PMID:22070522

26. Sumiyoshi K, Kubota S, Ohgawara T, Kawata K, Nishida T, Shimo T, Yamashiro T, Takigawa M. Identification of miR-1 as a micro RNA that supports late-stage differentiation of growth cartilage cells. Biochem Biophys Res Commun. 2010; 402:286–90. https://doi.org/10.1016/j.bbrc.2010.10.016 PMID:20937250

27. Yu HD, Xia S, Zha CQ, Deng SB, Du JL, She Q. Spironolactone regulates HCN protein expression through micro-RNA-1 in rats with myocardial infarction. J Cardiovasc Pharmacol. 2015; 65:587–92. https://doi.org/10.1097/FJC.0000000000000227 PMID:26065643

28. Heidersbach A, Saxby C, Carver-Moore K, Huang Y, Ang YS, de Jong PJ, Ivey KN, Srivastava D. microRNA-1 regulates sarcomere formation and suppresses smooth muscle gene expression in the mammalian heart. Elife. 2013; 2:e01323. https://doi.org/10.7554/eLife.01323 PMID:24252873

29. Chang J, Xu W, Du X, Hou J. MALAT1 silencing suppresses prostate cancer progression by upregulating miR-1 and downregulating KRAS. Onco Targets Ther. 2018; 11:3461–73. https://doi.org/10.2147/OTT.S164131 PMID:29942138

30. Li EY, Zhao PJ, Jian J, Yin BQ, Sun ZY, Xu CX, Tang YC, Wu H. Vitamin B1 and B12 mitigates neuron apoptosis in cerebral palsy by augmenting BDNF expression through MALAT1/miR-1 axis. Cell Cycle. 2019; 18:2849–59. https://doi.org/10.1080/15384101.2019.1638190 PMID:31500509

31. Li J, Peng J, Wang C, Deng H, Li Y. Calcitonin gene-related peptide suppresses isoprenaline-induced cardiomyocyte apoptosis through regulation of microRNA-1 and microRNA-133a expression. Zhong Nan Da Xue Xue Bao Yi Xue Ban. 2011; 36:964–71. https://doi.org/10.3969/j.issn.1672-7347.2011.10.006 PMID:22086007

32. Nicholls SJ, Pisaniello AD, Kataoka Y, Puri R. Lipid pharmacotherapy for treatment of atherosclerosis. Expert Opin Pharmacother. 2014; 15:1119–25. https://doi.org/10.1517/14656566.2014.904287 PMID:24702590

33. Draeger A, Monastyrskaya K, Mohaupt M, Hoppeler H, Savolainen H, Allemann C, Babiychuk EB. Statin therapy induces ultrastructural damage in skeletal muscle in patients without myalgia. J Pathol. 2006; 210:94–102. https://doi.org/10.1002/path.2018 PMID:16799920

34. Marcoff L, Thompson PD. The role of coenzyme Q10 in statin-associated myopathy: a systematic review. J Am Coll Cardiol. 2007; 49:2231–37. https://doi.org/10.1016/j.jacc.2007.02.049 PMID:17560286

35. Thompson PD, Parker B. Statins, exercise, and exercise training. J Am Coll Cardiol. 2013; 62:715–16. https://doi.org/10.1016/j.jacc.2013.03.030 PMID:23583256

36. Schirris TJ, Renkema GH, Ritschel T, Voermans NC, Bilos A, van Engelen BG, Brandt U, Koopman WJ, Beyrath JD, Rodenburg RJ, Willems PH, Smeitink JA, Russel FG. Statin-induced myopathy is associated with mitochondrial complex III inhibition. Cell Metab. 2015; 22:399–407. https://doi.org/10.1016/j.cmet.2015.08.002 PMID:26331605

37. Vrkić Kirhmajer M, Macolić Šarinić V, Šimičević L, Ladić I, Putarek K, Banfić L, Božina N. Rosuvastatin-induced rhabdomyolysis - possible role of ticagrelor and patients' pharmacogenetic profile. Basic Clin Pharmacol Toxicol. 2018; 123:509–18. https://doi.org/10.1111/bcpt.13035 PMID:29734517

SUPPLEMENTARY MATERIALS

Supplementary Methods

Reagents

Primary antibodies against Bcl-2 (ab196495, UK), Bax (ab32503, UK), were obtained from Abcam. Primary antibody against cleaved-caspase3 (#9661, USA), pro-caspase3 (#9662, USA), cleaved-caspase7 (#9491, USA), pro-caspase7 (#9492, USA), cleaved-caspase9 (#9509, USA), pro-caspase9 (#9504, USA) was purchased from Cell Signaling Technology. Primary α-tublin antibody was from Proteintech (11224-1-AP, China) and GAPDH antibody was from Servicebio (GB11002, China). Polyclonal antibodies against MAP3K1 was obtained from SANTA CRUZ (sc-449, USA). Dulbecco Modified Eagle Medium (DMEM) was obtained from Hyclone (SH30022.01B, USA). Fetal bovine serum (FBS) was purchased from Thermo Fisher Scientific (10099141C, USA). Reduced serum medium was from Thermo Fisher Scientific (11058021, USA). Horse serum was from Solarbio (S9050, China). Lipofectamine 3000 was obtained from Invitrogen (L3000015, USA). Simvastatin was from TargetMol (T0687, USA). Simvastatin concentrations were expressed as the final molar concentration in the buffer.

Isolation and differentiation of skeletal muscle satellite cells

Gastrocnemius muscle was isolated from 10 days old suckling mice (C57BL/6) and was cut into small pieces. Collagenase II and trypsin were used to digest muscle tissue at 37° C, and the impurities were removed by 200 mesh cell sieve. After centrifugation for 10 minutes at a speed of 1000 rpm, the cells were suspended in DMEM medium containing 10% fetal bovine serum, and then the cell suspension was placed in a culture flask. The culture flask was placed in an incubator containing 5% CO_2 at 37° C. Muscle satellite cells were isolated by using the difference of the adhesion speed with fibroblasts for a total of 30 min X 3 times. Cell suspension was extracted and placed in a culture flask. 1. 2×10^6 cells were seeded in each well of 6-well plate. When the cell density reached 80-90%, DMEM medium containing 10% fetal bovine serum was replaced with DMEM medium containing 2% horse serum. The medium was changed every day. After 3 days, the cells began to differentiate. After 5 days, 90% of satellite cells differentiated into mature skeletal muscle cells with the fusion of skeletal muscle cells into myotubes and MHC positive expression (Supplementary Figure 1).

Transfection of miR-1a mimics and inhibitor *in vitro*

After the muscle satellite cells were well differentiated, the culture medium was removed from 6-well cell culture cluster and washed cells three times with PBS. Mix the miR-1a mimics and inhibitor with the serum-free medium and Lipofectamine 3000 according to the protocol of Lipofectamine 3000. The concentration of inhibitor was 37.5 pmol/ml. 250μl of the mixture was added to each well of 6-well. After 4-6 hours, the reduced serum medium was changed to normal medium containing 10% FBS.

Mutagenesis of miR-1a binding sites in MAP3K1 mRNA 3′-UTR

These reporter constructs were generated in two steps. First, a coding-region fragment containing the miR-1a binding site was generated by PCR and cloned into the pMIR luciferase vector (Ambion) using SpeI and MluI cloning sites. Next, site-directed mutagenesis was performed, introducing three mutations into the binding site's seed sequence in MAP3K1 mRNA 3′-UTR. Subsequently, a DNA fragment containing the 3′-UTR miR-1a binding site was generated by PCR and cloned into pMIR vector, this time using MluI and HindIII sites.

Plasmid transfection into HEK293 and reporter assays

The plasmid constructs (MAP3K1-UTR or MT-MAP3K1-UTR) were co-transfected in HEK293 cells with the pCMV β-gal plasmid and 50 nM each of chemically synthesized miR-1a or negative control oligonucleotides (Applied Biosystems) by using lipofectamine 3000 (Invitrogen). Cells were harvested 48 hours after transfection, and luciferase and β-galactosidase activities were measured.

Construction and infection of lentivirus to cells or mice

The lentivirus construction compassing miR-1a was generated using the AdMax (Microbix) and pSilencer™ adeno 1.0-CMV (Ambion) systems according to the manufacturers' recommendations. Viruses were packaged and amplified in HEK293A cells and purified using CsCl banding followed by dialysis against 10 mM Tris-buffered saline with 10% glycerol. Titering

was performed on HEK293 cells using the Adeno-X Rapid Titer kit (BD Biosciences Clontech, Palo Alto, CA, USA) according to the manufacturer's instructions. MiR-1a mimics sequence: 5′-3′ UGGAAUGUAAAGAAGUAUGUAU/ 5′-3′ ACAUACUUCUUUACAUUCCAUU. miR-1a inhibitor sequence: 5′-3′ AUACAUACUUCUUUAC AUUCCA. Cells were infected with lentivirus overnight in antibiotics-free medium supplemented with 2% FBS. The cells were then washed and incubated in fresh medium for an additional 12 hours before experimentation. For infecting mice, lentivirus containing miR-1a inhibitor sequence or control was injected via tail vein under pressure (in 1 ml of PBS over 5-10s). Lentivirus was injected via tail vein in 100 μl of PBS with 7.6×10^7 IFUs of loaded lentivirus. The concentration of miR was 10 mg/kg.

RNA quantification

Total RNA was isolated using a TRIzol-based (Invitrogen) RNA isolation protocol. RNA was quantified by Nanodrop (Agilent Technologies), and RNA and miRNA quality were verified using an Agilent 2100 Bioanalyzer (Agilent Technologies). Samples required 260/280 ratios of more than 1.8, and sample RNA integrity numbers of more than 9 for inclusion. RNA was reverse transcribed using the TaqMan microRNA Reverse Transcription Kit (Applied Biosystems) according to the manufacturer's instructions. Reactions were run for 40 cycles at conditions according to the manufacturer's protocol. U6 was used as a control gene and the target values were normalized to U6 mRNA. miR-1a primer sequences: 5′-GCCGAATGGAATGTAAAGAAGT-3′/5′-TATGGT TTTGACGACTGTGTGAT-3′. MAP3K1 primer sequences: 5′-GTGGTGAAGCCAATCCCTATTA-3′/5′-CTGTCTCCTCCAATCAGGAAAG-3′. U6 primer sequences: 5′-CAGCACATATACTAAAAT TGGAACG-3′/5′-ACGAATTTGCGTGTCATCC-3′. The fold change was calculated using the 2-DD computed tomography method.

Western blotting

Cells or tissues were homogenized on ice in cell-lysis buffer (20 mM Tris-HCl, pH 7.5, 150 mM NaCl, 1 mM Na_2EDTA, 1 mM EGTA, 1% Triton, 2.5 mM sodium pyrophosphate, 1 mM beta-glycerophosphate, 1 mM Na_3VO_4, 1 μg/ml leupeptin) and 1 mM PMSF. Cell was lysated with cell-lysis buffer. The protein content was assayed by BCA protein assay reagent (Pierce, USA). 20 μg proteins were loaded to SDS-PAGE and then transferred to membrane. Membrane was incubated with a 1:1000 dilution of primary antibody, followed by a 1:2000 dilution of horseradish peroxidase- conjugated secondary antibody. Protein bands were visualized by ECL (GE Healthcare). The intensity (area X density) of the individual bands on Western blots was measured by densitometry (model GS-700, Imaging Densitometer; Bio-Rad). The background was subtracted from the calculated area. We used control as 100%.

Immunohistochemistry

The tissue was fixed in 4% paraformaldehyde overnight, and then processed, embedded in paraffin, and sectioned at 4 μm. The deparaffinized, rehydrated section (5 μm) were microwaved in citrate buffer for antigen retrieval. Sections were incubated in endogenous peroxidase (DAKO) and protein block buffer, and then with primary antibodies indicated overnight at 4° C. Slides were rinsed with washing buffer and incubated with labelled polymer-horseradish peroxidase-antimouse/antirabbit antibodies followed by DAB^+ chromogen detection (DAKO). After final washes, sections were counterstained with hematoxylin. All positive staining was confirmed by ensuring that no staining occurred under the same conditions with the use of non-immune rabbit or mouse control IgG.

TUNEL assay

When the cell differentiation on the glass sheet was completed, the glass sheet was removed from the culture medium and fixed in 4% formaldehyde solution for 30 minutes after washing with PBS once. Then, the glass sheets were placed in PBS containing 0.3% Triton X-100 and incubated at room temperature for 5 minutes. TUNEL detection solution according to the instructions of Fluorescent TUNEL Apoptosis Detection Kit (Beyotime, C1088, China) was prepared and mixed well. 50μl of TUNEL detection solution was added to the sample and incubated for 60 minutes in the dark at 37° C. The sheets were sealed with anti-fluorescence quenching solution and observed under fluorescence microscope (Olympus, Japan). The excitation wavelength used ranged from 450 to 500 nm and the emission wavelength ranged from 515 to 565 nm (green fluorescence).

Flow cytometry

Cells were exfoliated with EDTA-free trypsin and transferred to specific tubes for flow cytometry. The cells were treated and dyed according to the procedure recommended by Annexin V PE Apoptosis kit (BD, 559763, USA). The processed samples were kept away from light and detected by flow cytometer (BD, FACS ARIA2, USA) within 1 hour.

Cell counting kit-8 (CCK8) assay

Cells were seeded in 96-well plates and differentiated into mature skeletal muscle cells. Skeletal muscle cells were stimulated according to pre-designed conditions, and appropriate amount of CCK8 (BOSTER, AR1160, China) solution was added to 96-well plates, incubated in a cell incubator containing 5% CO_2 at 37° C for 1 hour. The absorbance was measured at 450 nm wavelength.

Detection of serum myotoxicity markers

Serum creatine kinase (CK) and lactate dehydrogenase (LDH) in mice were detected as indicators of myotoxicity. Creatine Kinase Assay Kit (Nan Jing Jian Cheng Bioengineering Institute, A032-1-1, China) and Lactate Dehydrogenase Assay Kit (Nan Jing Jian Cheng Bioengineering Institute, A020-1-2, China) was used for the detection. Absorbance was measured at 660 nm and 440 nm wavelength, respectively.

Hanging grid test

The hanging grid test was performed at the end of experiment. Mice were individually placed at the center of a wiremesh screen (2 mm wire thickness). The screen was held 50 cm above a pad. The grid was inverted upside down with the head declining first. The duration of hanging was recorded in three independent trials conducted at least 20 min apart. The data of all three trials were averaged.

Forelimb grip strength test

At the end of experiment, a forelimb grip strength test was performed using a grip strength metre (Handpi HP-5N, China). Mice were held by the tail and grasped a grid with fore paws. The mice were gently pulled by the tail until they released their grip. The forces from three trials were recorded and averaged.

Running tolerance test

Running tolerance test was performed at the end of experiment. The running speed was started at 13 m/min and increased 2 m/min every 3 min. The slop of track was started at 0° C, increased 2° C every 3 min, and maintained at 14° C because of limit of the treadmill. No warm-up was provided before the assessment of running tolerance. The time and distance were recorded when the mice were exhausted.

Hematoxylin eosin stain

Gastrocnemius was fixed in 4% paraformaldehyde for 24 h. Subsequently, the fixed muscles were dehydrated through an ethanol series, treated with xylenes, embedded in paraffin sections, and cut into 5 μm sections. Dewaxing was performed through xylene and ethanol series to deionized water. Stain the nuclei with haematoxylin for 3 min and differentiate with acid ethanol for 30 s. Rinse in the running water until blue up. Then the slides were stained with eosin for 2 min. Dehydrate the slides through ethanol, clear in xylene, and mount. The imaging was performed using Olympus DP72 digital imaging system (Olympus Corporation, Tokyo, Japan). Cross-sectional area (CSA) of muscle fibres was measured using Image Pro Plus. The analysis of CSA was conducted by single investigator blinded to sample.

Statistical analysis

All quantitative results are expressed as mean ± s.e.m. A one-way ANOVA followed by Tukey *post-hoc* tests was used to determine *P* value. Statistical analysis was conducted using IBM SPSS statistics 20.0 (IBM Corp., Armonk, NY, USA) and $P<0.05$ were considered as statistical significance.

Supplementary Figures

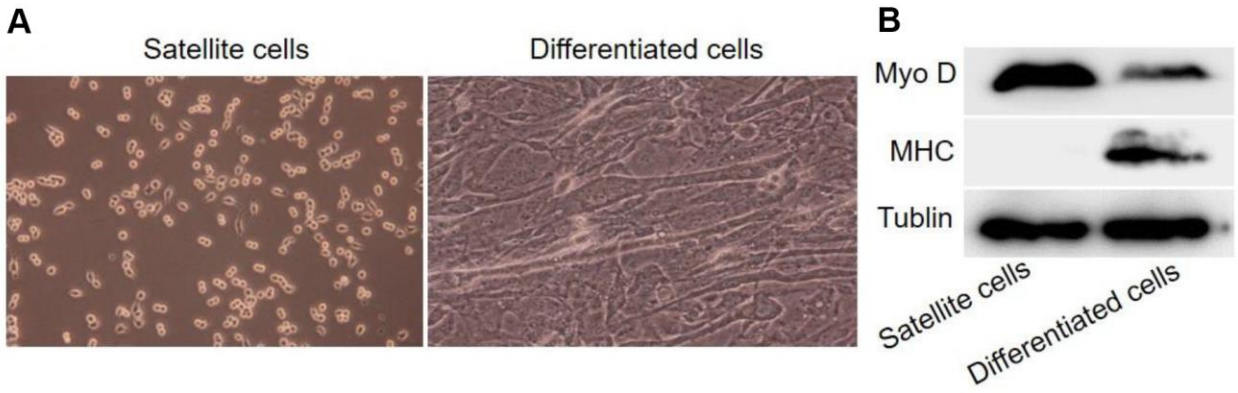

Supplementary Figure 1. Differentiation of skeletal muscle satellite cells to skeletal muscle cells. (**A**) Primary skeletal muscle satellite cells and differentiated skeletal muscle satellite cells with the formation of myotubes. (**B**) Skeletal muscle cells were identified using western blot. MyoD is a biomarker of skeletal muscle satellite cells. MHC is a biomarker of skeletal muscle cells.

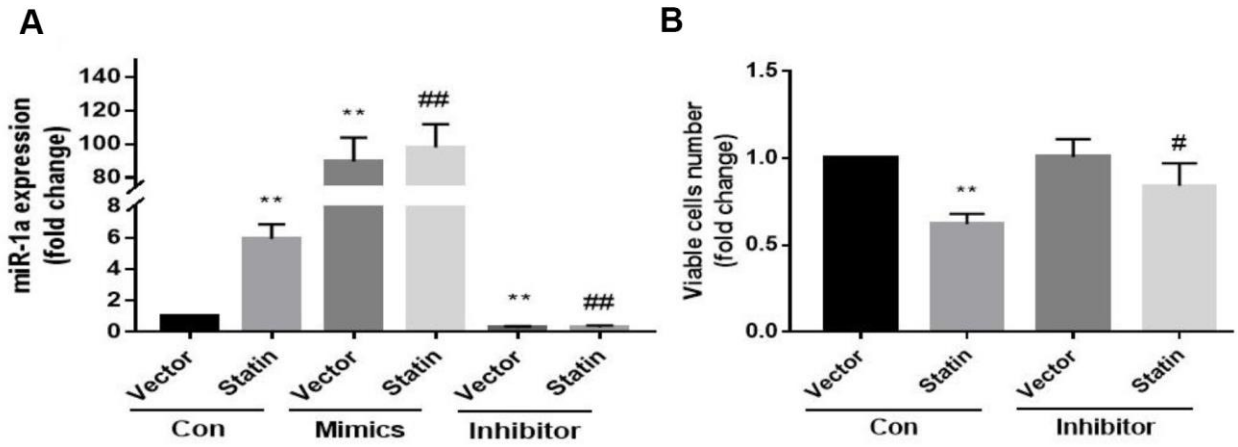

Supplementary Figure 2. Downregulation of miR-1a increases cell viability in skeletal muscle cells treated with statin. (**A**) Cultured skeletal muscle cells were transfected with miR-1a mimics and inhibitor for 48 hours followed by statin treatment for 24 hours. Cells were subjected to detect the levels of miR-1a using real-time PCR. N is 5 in each group. $^{**}P<0.01$ vs. vector alone. $^{\#\#}P<0.01$ vs. statin alone. (**B**) Cultured skeletal muscle cells were transfected with miR-1a inhibitor for 48 hours followed by statin treatment for 24 hours. Cell viability was determined by CCK8 method. N is 5 in each group. $^{**}P<0.01$ vs. vector alone. $^{\#}P<0.05$ vs. statin alone. A one-way ANOVA followed by Tukey *post-hoc* tests was used to determine *P* value in (**A**, **B**).

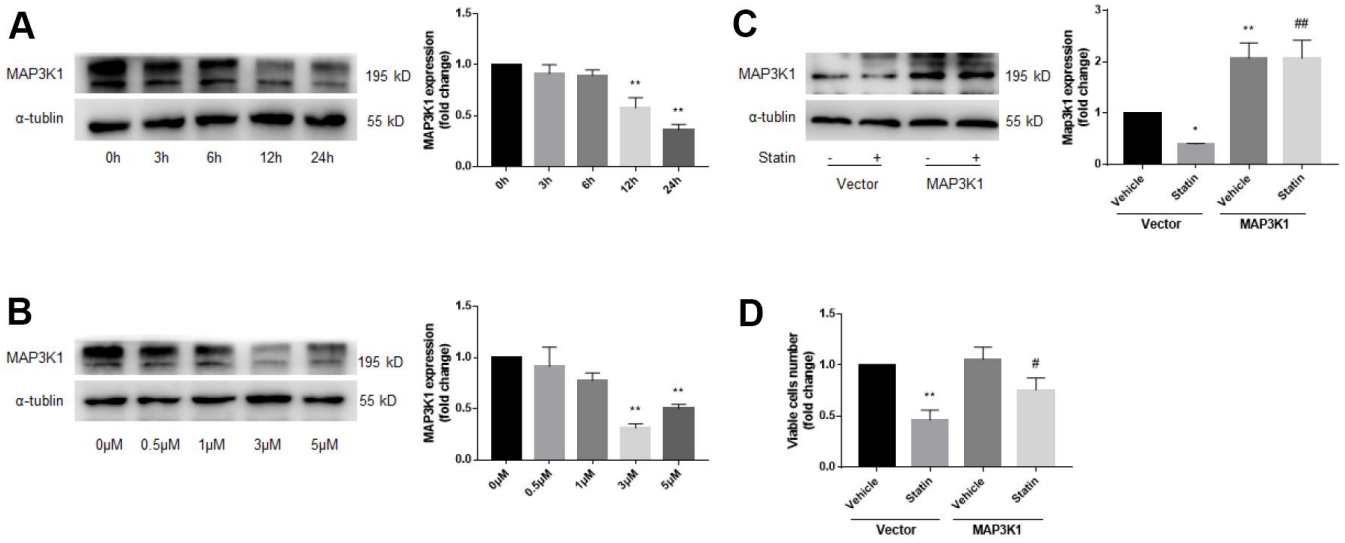

Supplementary Figure 3. Statin reduces the expression of MAP3K1 protein in skeletal muscle cells and MAP3K1 overexpression increases the number of viable cells under statin stimulation. (**A**) Cultured skeletal muscle cells were treated with simvastatin (5 μM) as indicated time points. The expressions of MAP3K1 protein was assayed using western blot. N = 5 per group. $^{**}P < 0.01$ vs. control group (0 h). (**B**) Cultured skeletal muscle cells were treated with simvastatin (24 hours) as indicated concentration points. The expressions of MAP3K1 protein was assayed using western blot. N = 5 per group. $^{**}P < 0.01$ vs. control group (0 μM). (**C**, **D**) Cultured skeletal muscle cells were transfected with plasmids MAP3K1 cDNA for 48 hours followed by statin treatment for 24 hours. Cells were subjected to detect the protein levels of MAP3K1 by western blot in (**C**). Viable cell numbers were determined by the CCK8 method in (**D**) N = 5 per group. $^{**}P < 0.01$ vs. vector alone. $^{\#}P < 0.05$ or $^{\#\#}P < 0.01$ vs. statin alone. A one-way ANOVA followed by Tukey *post-hoc* tests was used to determine *P* value in (**A**–**D**).

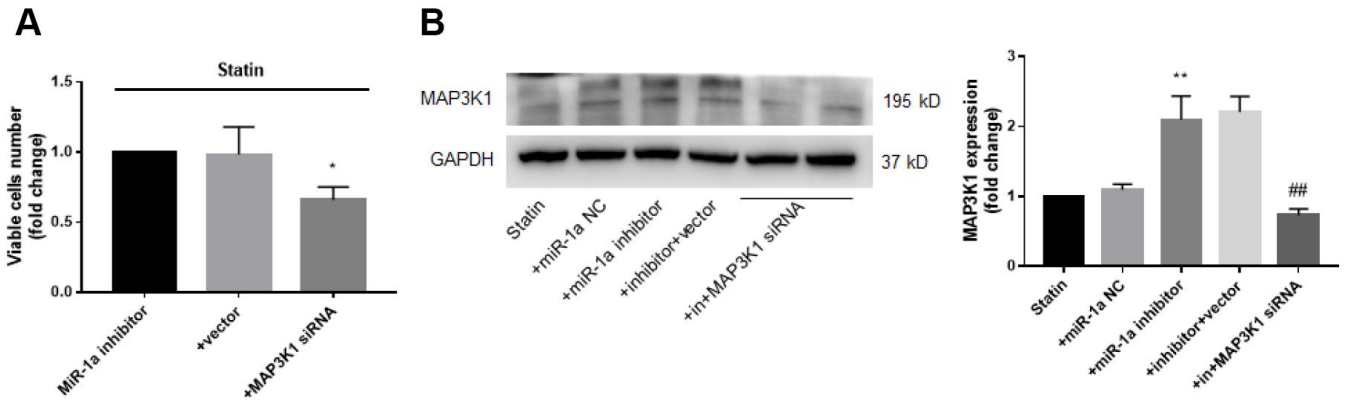

Supplementary Figure 4. The miR-1a-MAP3K1 pathway mediates statin-induced reduction in viable skeletal muscle cell number. Cultured skeletal muscle cells were transfected with miR-1a inhibitor and/or MAP3K1 siRNA for 48 hours followed by statin treatment for 24 hours. (**A**) Viable cell numbers were determined by the CCK8 method. N = 5 per group. $^{*}P < 0.05$ vs. statin+miR-1a inhibitor. (**B**) Cells were subjected to detect the protein levels of MAP3K1. N = 5 per group. $^{**}P < 0.01$ vs. statin alone. $^{\#\#}P < 0.01$ vs. statin+miR-1a inhibitor. A one-way ANOVA followed by Tukey *post-hoc* tests was used to determine *P* value in (**A**, **B**).

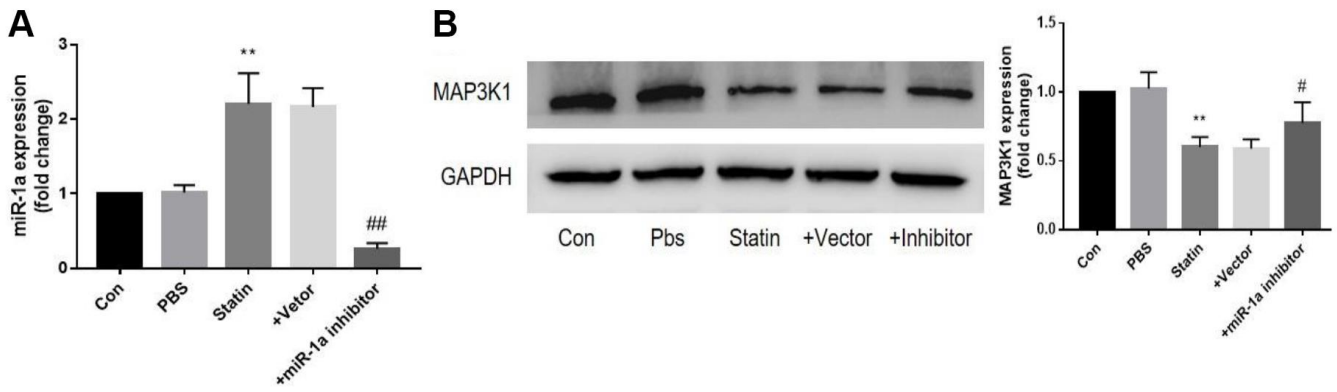

Supplementary Figure 5. Statin decreases the expression of MAP3K1 protein through miR-1a *in vivo*. The protocol for animal experiments was shown in Figure 6A. (**A**) The levels of miR-1a were assayed using real-time PCR. (**B**) The expressions of MAP3K1 protein was assayed using western blot. N is 10-15 in each group. $^{**}P < 0.01$ vs. PBS group. $^{\#}P<0.05$ or $^{\#\#}P<0.01$ vs. statin alone. A one-way ANOVA followed by Tukey *post-hoc* tests was used to determine *P* value in (**A**, **B**).

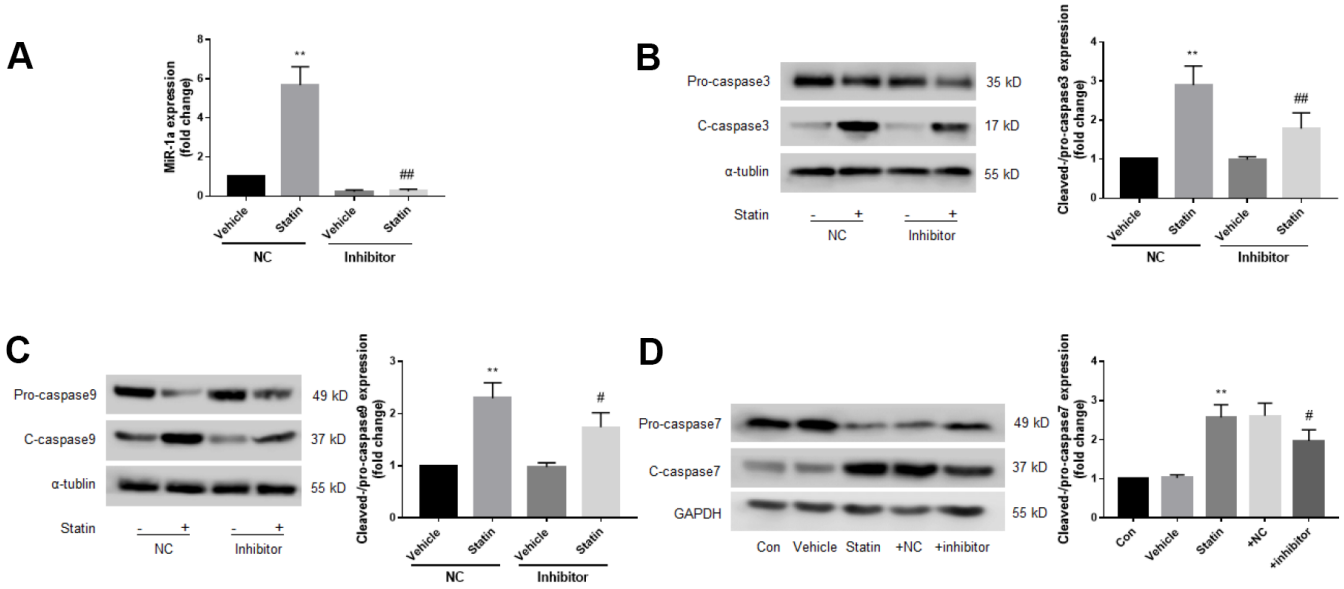

Supplementary Figure 6. Pravastatin (hydrophilic) increases the miR-1a expression in skeletal muscle cells, and inhibition of miR-1a ameliorates statin-induced cell apoptosis. Cultured skeletal muscle cells were transfected with miR-1a inhibitors for 48 hours followed by statin treatment for 24 hours. (**A**) The expression of miR-1a was determined by PCR. (**B**–**D**) Cells were subjected to detect the protein levels of pro-/cleaved-caspase3 in (**B**) pro-/cleaved-caspase9 in (**C**) and pro-/cleaved-caspase7 in (**D**) by western blot. N is 5 in each group. $^{**}P<0.01$ vs. NC alone. $^{\#}P<0.05$ or $^{\#\#}P<0.01$ vs. statin alone. A one-way ANOVA followed by Tukey *post-hoc* tests was used to determine *P* value in (**A**–**D**).

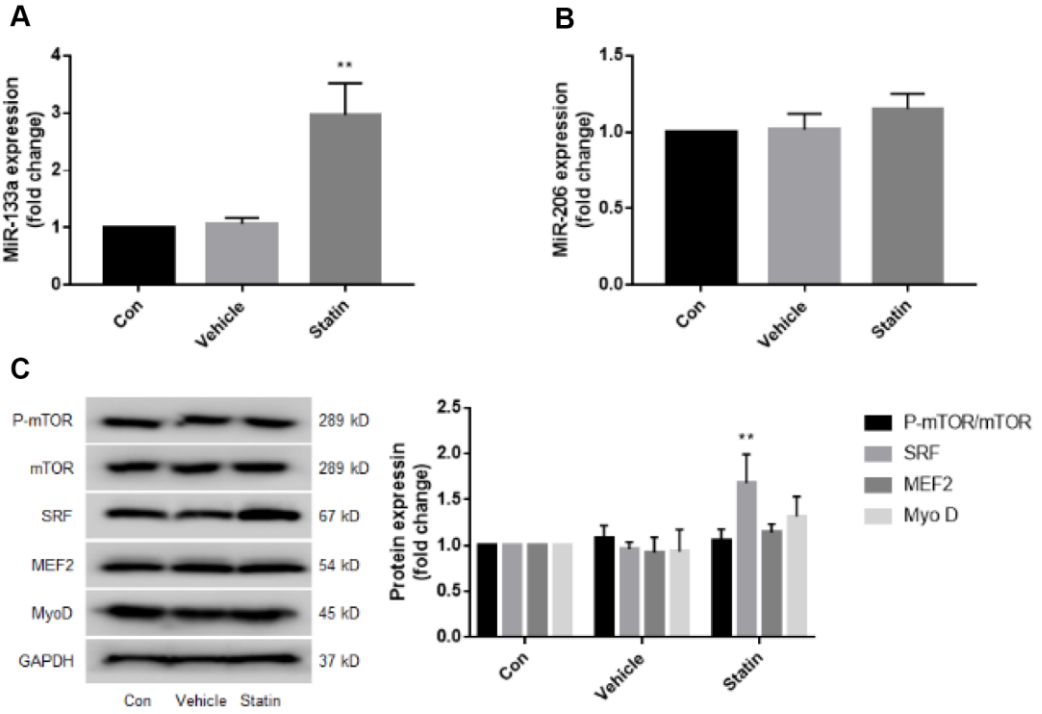

Supplementary Figure 7. After simvastatin stimulation, the expression of miR-133a, SRF increased, while the expression of miR-206, mTOR, MEF2, MyoD did not change significantly. Cultured skeletal muscle cells were stimulated by statin for 24 hours. (**A**, **B**) Cells were subjected to detect the levels of miR-133a in (**A**) and miR-206 in (**B**) by PCR. N is 5 in each group. $^{**}P<0.01$ vs. vehicle alone. (**C**) Cells were subjected to detect the protein levels of mTOR, SRF, MEF2, MyoD by western blot. N is 5 in each group. $^{**}P<0.01$ vs. vehicle alone. A one-way ANOVA followed by Tukey *post-hoc* tests was used to determine *P* value in (**A**–**C**).

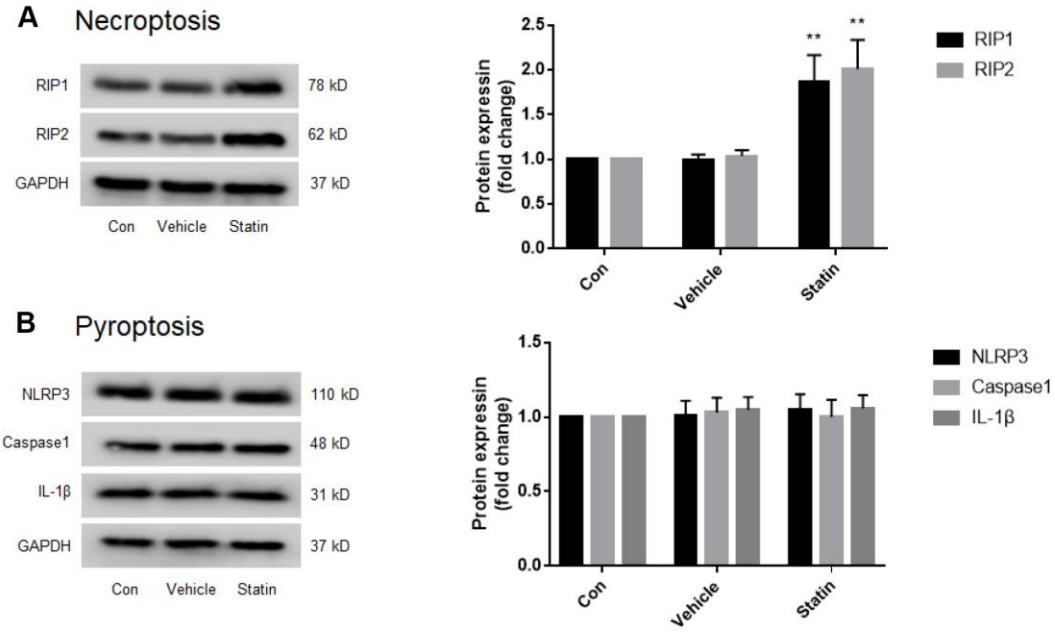

Supplementary Figure 8. Under simvastatin stimulation, the level of necroptosis was significantly increased, while the level of pyroptosis was not. Cultured skeletal muscle cells were stimulated by statin for 24 hours. Cells were subjected to detect the protein levels of RIP1 and RIP2 in (**A**) and NLPP3, caspase1 and IL-1β in (**B**) by western blot. N is 5 in each group. $^{**}P<0.01$ vs. vehicle alone. A one-way ANOVA followed by Tukey *post-hoc* tests was used to determine *P* value in (**A**, **B**).

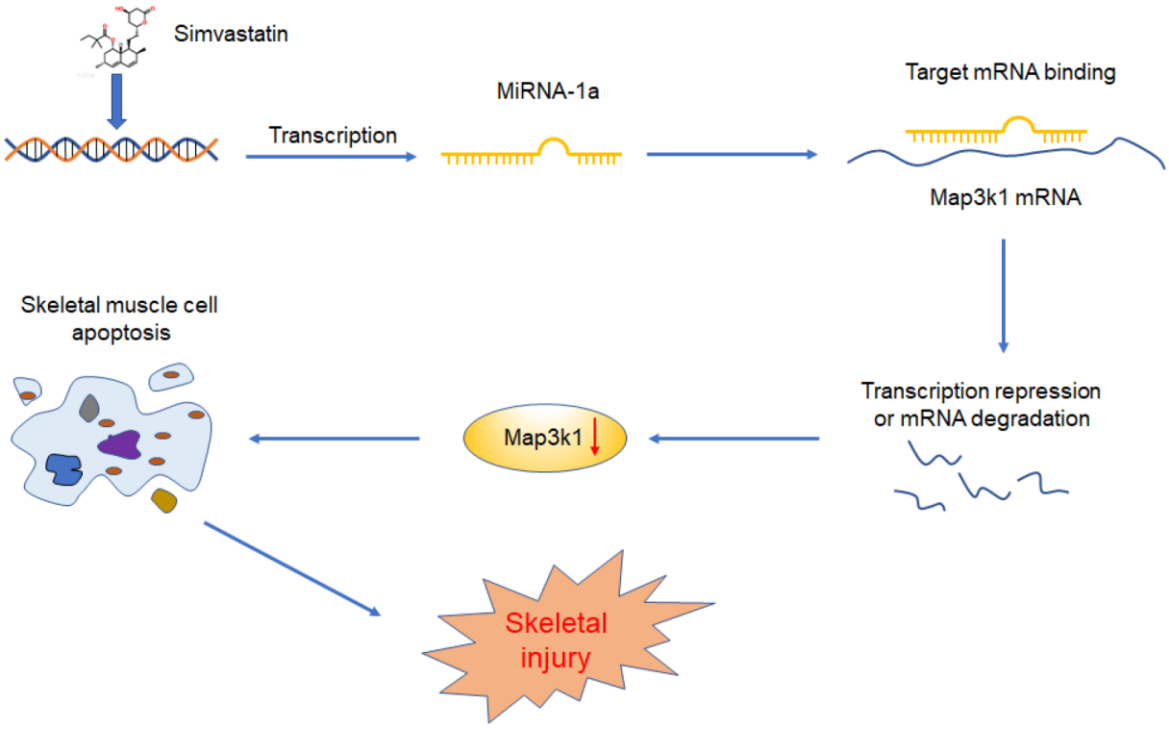

Supplementary Figure 9. Proposed mechanism of statin inducing skeletal myopathy. Statin therapy induces miR-1a excessively expressed in skeletal cells. MiR-1a inhibits MAP3K1 gene expression by targeting 3'-UTR of MAP3K1 mRNA, resulting in apoptosis of skeletal muscle cells. In this way, statin causes skeletal myopathy.

Supplementary Tables

Supplementary Table 1. Body weight of mice in each group (g).

Group	-2 w	-1 w	0 w	1 w	2 w	3 w	4 w	5 w	6 w	7 w	8 w
Con	16.3±3.4	16.9±2.8	17.8±3.0	19.4±3.2	21.8±2.9	22.4±3.5	23.9±4.1	24.6±3.7	26.4±4.6	27.8±4.3	29.6±4.5
Vehicle	16.1±2.9	17.2±3.1	17.6±3.2	18.9±2.9	20.5±3.4	22.3±3.3	24.2±3.9	24.7±3.9	25.9±4.2	26.7±4.2	28.4±4.7
Statin	16.2±3.1	16.8±2.7	17.5±2.7	18.2±2.7	18.4±2.5	19.7±2.3	20.2±2.5*	21.7±3.0	22.5±3.1	22.8±3.3*	23.3±3.2*
+NC	16.5±2.2	16.9±2.9	17.8±2.5	18.5±3.3	18.7±2.9	19.5±2.8	20.5±2.3	21.3±2.9	21.8±3.2	22.3±3.0	23.1±3.1
+inhibitor	16.2±3.1	17.0±2.8	17.6±2.9	18.1±2.8	18.6±2.3	20.3±2.2	21.7±2.1	22.9±2.2	24.4±3.0	25.2±3.1	26.9±3.5

*P<0.05 vs. vehicle group.

Supplementary Table 2. Food intake of mice in each group (g/day/mouse).

Group	-2 w	-1 w	0 w	1 w	2 w	3 w	4 w	5 w	6 w	7 w	8 w
Con	3.1±0.4	3.7±0.5	4.2±0.6	4.8±0.5	5.2±0.6	5.4±0.7	5.8±0.7	6.3±0.8	6.8±1.1	7.3±0.8	7.5±1.2
Vehicle	3.2±0.6	3.6±0.8	4.1±0.5	5.0±0.7	5.3±0.6	5.5±0.6	5.7±0.8	6.2±0.7	6.5±0.9	7.1±1.0	7.4±0.9
Statin	3.1±0.5	3.5±0.6	4.1±0.6	4.9±0.7	5.1±0.5	5.2±0.7	5.2±0.6	5.7±0.5	5.9±0.6	6.0±0.6**	6.2±0.8**
+NC	3.0±0.4	3.6±0.6	3.9±0.5	4.8±0.6	5.2±0.7	5.1±0.5	5.3±0.7	5.6±0.6	5.7±0.5	6.2±0.5	6.1±0.7
+inhibitor	3.1±0.7	3.5±0.7	4.0±0.4	4.7±0.5	5.3±0.6	5.4±0.6	5.4±0.5	6.0±0.7	6.1±0.8	6.6±0.9	6.9±0.7

**P<0.01 vs. vehicle group.

Supplementary Table 3. Serum total cholesterol concentrations of mice in each group (mmol/L).

Group	0w	8w
Con	14.5±2.4	15.3±2.8
Vehicle	14.2±3.1	14.7±2.9
Statin	15.6±2.6	10.4±1.2 **
+NC	14.3±2.4	10.9±1.7
+inhibitor	14.8±2.9	11.5±1.3

**P<0.01 vs. vehicle group.